

# Solution of Master and Fokker-Planck Equations by Propagator Methods, Applied to Au/NaCl Thin Film Nucleation

J. B. ADAMS

*Materials Science Program, University of Wisconsin-Madison,  
Madison, Wisconsin 53706*

AND

W. N. G. HITCHON

*Department of Electrical and Computer Engineering, University of Wisconsin-Madison,  
Madison, Wisconsin 53706*

Received March 6, 1987, revised June 19, 1987

Novel numerical solutions of Master and Fokker-Planck equations are described and compared for equivalent discrete and continuous problems. The two methods involve the calculation of long-time-step propagator matrices, whose single application is equivalent to many iterations of a finite difference scheme. For the discrete method we present two analytic propagators which are exact for growth-only (no decay) processes, and two approximate propagators for growth and decay processes. The continuous method couples a discrete boundary condition for small clusters with an efficient continuous description for large clusters. These two methods are applied to the nucleation and growth of vapor-deposited thin films whose atoms cluster together to form islands (Volmer-Weber growth). Mobility coalescence of islands is included to show how "slow" nonlinear processes may be included in the model. © 1988 Academic Press, Inc

## I. INTRODUCTION

An enormous variety of systems of interest in the physical, biological, and social sciences may be described by means of Master or rate equations. A typical example for describing the nucleation and growth of thin films is

$$\frac{dN_i}{dt} = -(G_i + D_i) N_i(t) + G_{i-1} N_{i-1}(t) + D_{i+1} N_{i+1}(t)$$

where  $N_i$  is the number of clusters of  $i$  atoms,  $G_i$  is the growth rate of clusters from  $i$  atoms to  $i+1$  atoms, and  $D_i$  is the decay rate of clusters from  $i$  atoms to  $i-1$  atoms by emission of atoms. To solve for a distribution of cluster sizes ranging from 1 to 10,000 atoms per cluster, one would solve 10,000 individual coupled rate equations, one for each cluster size

This Master equation approach is extremely powerful because it accurately models individual physical processes. However, the approach is limited by its excessive computational requirements, because the equations are coupled and must be solved iteratively, which could require thousands of iterations. The purpose of this paper is to show how to calculate long time-step propagator matrices which allow these extreme computational requirements to be greatly reduced for many classes of both discrete and continuous problems.

In Section II, we discuss discrete propagator methods and give a simple example using an explicit finite difference scheme. We then present four propagator methods which are far more efficient than finite-difference methods for many problems.

In Section III, we discuss propagator methods for continuous systems. We show how it is possible to transform discrete Master equations into equivalent continuous Fokker-Planck equations [1-6]. A continuous description of a discrete process usually allows an increased numerical efficiency while sacrificing some degree of accuracy. We present a simple scheme for taking large time-steps which greatly increases numerical efficiency in many systems.

In Section IV, we apply the discrete and continuous methods to a standard problem in thin film nucleation, the deposition of Au onto NaCl where the Au atoms cluster together to form islands. A novel and highly accurate method for calculating the boundary conditions is discussed. The results of the discrete and continuous methods are nearly identical, and the continuous method is significantly more efficient.

Section V describes how to include slow physical processes, such as the coalescence of two islands into a single larger one. Mobility coalescence has not been included in previous calculations, except in the case of small clusters [7]. Coalescence is a highly nonlinear process, but it acts on a time scale much slower than that of the capture of individual atoms, so it may be treated as a perturbation on the propagator methods. This method is then applied to the nucleation and growth of Au/NaCl, in which mobility coalescence of Au clusters is important.

## II. PROPAGATORS FOR DISCRETE SYSTEMS

A propagator is a Green's function which, when applied to a function, propagates that function forward in time. A propagator matrix describes the time evolution of each part of a vector. For example,

$$\bar{N}_i(t_0 + \tau) = \sum_j T_{ij}(\tau) \bar{N}_j(t_0), \quad (1)$$

where  $\bar{N}_i(t)$  is a vector specifying the numbers of clusters of each size,  $i$ , at time  $t$ , and  $\bar{T}_{ij}(\tau)$  is a propagator matrix corresponding to a time step of  $\tau$ . Repeated applications of the matrix can propagate the vector to any future time. The purpose of this paper is to show how to calculate accurate propagator matrices which allow large time-steps.

In general, it is a straightforward matter to calculate a sufficiently accurate propagator matrix for use in the numerical scheme. A simple example of generating a propagator matrix is by application of an explicit finite difference scheme, where the differencing is done with respect to time. For a growth-only process, the equations are

$$\frac{dN_i}{dt} = -G_i N_i(t) + G_{i-1} N_{i-1}(t) \quad (2)$$

$$N_i(t_0 + \tau) \approx N_i(t_0) + \tau \left. \frac{dN_i}{dt} \right|_{t=t_0} \quad (3)$$

Combining Eqs. (2) and (3) yields

$$N_i(t_0 + \tau) \approx N_i(t_0)[1 + \tau(-G_i)] + N_{i-1}(t_0)[\tau G_{i-1}]. \quad (4)$$

This yields a propagator matrix  $\bar{T}_i(\tau)$ , which satisfies Eq (1) and which can be rewritten as

$$N_i(t_0 + \tau) = T_{ii}(\tau) N_i(t_0) + T_{i, i-1}(\tau) N_{i-1}(t_0) = \sum_j T_{ij}(\tau) N_j(t_0), \quad (5)$$

where

$$\begin{aligned} T_{ii}(\tau) &= 1 - \tau G_i \\ T_{i, i-1}(\tau) &= \tau G_{i-1} \\ T_{ij}(\tau) &= 0 \quad \text{for } j \neq i, i-1. \end{aligned} \quad (6)$$

In other words,  $T_{ij}(\tau)$  is the fraction of the function at  $i$  at time  $t_0$  that has propagated to  $j$  at time  $t_0 + \tau$ . This finite difference method, cast in propagator matrix form, is valid only for a small time-step  $\tau$ ; as  $\tau$  increases, so does the error. For example, if the growth rates are equal and are such that 10% of the function propagates from  $i$  to  $i+1$  during time  $\tau$ , then approximately ( $\frac{1}{2} \times 10\% =$ ) 5% of the function at  $i+1$  should continue to propagate to  $i+2$ ; since the finite difference scheme does not allow for 2-grid-space propagation, it would be in error by approximately ( $5\% \times 10\% =$ ) 0.5% at  $i+2$ .

The propagator methods to be discussed overcome this limitation by allowing the function to propagate to *any* grid point. During the time of propagation, the rate equations are assumed to be linear so that the principle of superposition may be used. In other words, the propagation of each part of the function is calculated independently of the change of the rest of the function. This is a good approximation if and only if the propagation of the function only slightly changes the growth and decay rates. Thus, it is possible to solve nonlinear equations by assuming they are linear during a small time-step  $\tau$ .

We present four propagator methods for four different cases: growth-only processes with equal growth rates; growth-only processes with non-equal growth

rates; growth and decay processes with constant or slowly varying growth and decay rates; and general growth and decay processes.

*Case 1. Equal Growth Rates.* For growth-only processes, it is straightforward to construct exact propagator matrices. If the growth rates  $G_i$  are equal for all  $i$  and constant in time, then the propagation of the function at  $i$  to all  $j > i$  is found by solving

$$\begin{aligned} \frac{dN_i}{dt} &= -GN_i(t) + GN_{i-1}(t) \\ \frac{dN_{i+1}}{dt} &= -GN_{i+1}(t) + GN_i(t) \\ &\vdots \\ \frac{dN_k}{dt} &= -GN_k(t) + GN_{k-1}(t). \end{aligned} \tag{7}$$

If we consider only the propagation from  $N_i(t_0)$ , then the boundary conditions are  $N_{k \neq i}(t_0) = 0$  and  $N_i(t_0) = N_i(t_0)$ , yielding

$$\begin{aligned} n_{ii}(t_0 + \tau) &= N_i(t_0) e^{-G\tau} \\ n_{i+k,i}(t_0 + \tau) &= N_i(t_0) \frac{G^k \tau^k}{k!} e^{-G\tau}, \end{aligned} \tag{8}$$

where  $n_{i+k,i}$  is the part of the function which has propagated from  $i$  to  $i+k$  after a time-step  $\tau$ .

Let us now consider a different set of boundary conditions, where  $N_k(t_0) \neq 0$ . By using the principle of superposition, we can use the above result to individually calculate the propagation of each part of the function, and then sum the results of the propagation. The result is

$$N_j(t_0 + \tau) = \sum_{i < j} n_{ji}(t_0 + \tau). \tag{9}$$

By comparison with Eq. (1), we find

$$\begin{aligned} T_{ii}(\tau) &= \exp(-G\tau) \\ T_{i+k,i}(\tau) &= \frac{G^k \tau^k}{k!} e^{-G\tau}. \end{aligned} \tag{10}$$

Thus, we have found an exact propagator matrix for growth-only processes with equal growth rates.

*Case 2. Non-Equal Growth Rates.* It is also possible to find an exact propagator for growth-only processes with non-equal rates ( $G_i \neq G_j$ ), which are

constant in time. This calculation was inspired by a paper by Zinsmeister [8] and is similar to the above calculation for constant growth rates. The rate equations to be solved are

$$\begin{aligned} \frac{dN_i}{dt} &= -G_i N_i(t) + G_{i-1} N_{i-1}(t) \\ &\vdots \\ \frac{dN_k}{dt} &= -G_k N_k(t) + G_{k-1} N_{k-1}(t). \end{aligned}$$

As in Case 1, we use the principle of superposition, which yields

$$\begin{aligned} T_u(\tau) &= \exp(-G_i \tau) \\ T_{i+j,i}(\tau) &= \sum_{k=0}^j C_{i+k}^{i+j} e^{-G_{i+k} \tau}, \end{aligned} \tag{11}$$

where

$$\begin{aligned} C_{i+k}^{i+j} &= 1 && \text{for } j = k = 0, \\ &= \frac{G_{i+j-1}}{G_{i+j} - G_{i+k}} C_{i+k}^{i+j-1} && \text{for } k \neq j, \\ &= - \sum_{s=0}^{k-1} C_{i+s}^{i+j} && \text{for } k = j \neq 0 \end{aligned} \tag{12}$$

Thus, for a growth-only system, we can calculate a propagator for either equal growth rates (EGR) or non-equal growth rates (NEGR). Both propagators are *exact* for *any* size time-step. However, if one has nearly equal growth rates in the NEGR method, one must retain many significant figures, especially for large time-steps. This can be seen by inspection of Eqs. (11) and (12); when growth rates are nearly equal, the  $C_{i+k}^{i+j}$  become enormous, yet their summation in Eq. (11) must yield a  $T_{i+j,i}$  between 0 and 1. The number of retained significant figures therefore limits the allowed time step of the NEGR method. Of course, for very nearly equal growth rates, the EGR method would be a good approximation, especially if  $G$  is appropriately averaged.

*Case 3. Haken's Method.* A better method for treating birth and death processes was presented by Haken [9]. He derived a propagator matrix which for one dimension can be written in the form

$$T_{j,i}(\tau) = \frac{\exp\left(-\frac{(j-i - K_i \tau)^2}{2Q_i \tau}\right)}{\sqrt{2\pi Q_i \tau}}, \tag{13}$$

where  $K$ , the drift term, and  $Q$ , the diffusion term, are defined by

$$\begin{aligned} K_i &= G_i - D_i \\ Q_i &= G_i + D_i. \end{aligned} \tag{14}$$

This method is inaccurate for small  $\tau$ , but becomes increasingly accurate for large  $\tau$ , provided that  $K$  and  $Q$  are constant independent of  $i$  and time (see Fig. 1).

If  $K$  and  $Q$  vary slowly, then it is possible to use a propagator developed by Wissel for continuous problems [10] This propagator matrix has the form

$$T_{ij}(\tau) = \frac{\exp\left(-\alpha\tau\left(\frac{\partial K_j}{\partial x} - \frac{1}{2}\frac{\partial^2 Q_j}{\partial x^2}\right)\right)}{\sqrt{2\pi\tau(\alpha Q_j + \beta Q_i)}} \exp\left(-\frac{\left(j-i - \tau(\alpha K_j + \beta K_i) - \alpha\frac{\partial Q_i}{\partial x}\right)^2}{2\tau(\alpha Q_j + \beta Q_i)}\right), \tag{15}$$

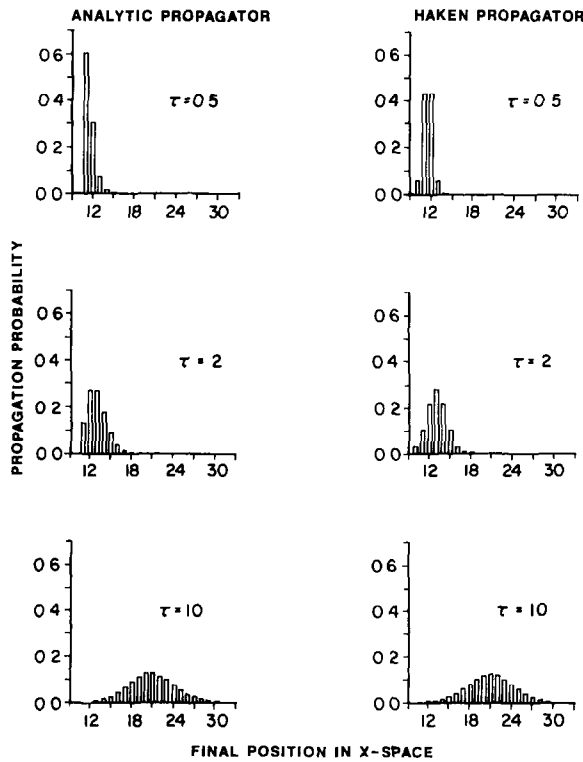


FIG 1 An initial histogram of height 1 at  $x=11$  is propagated for different time-steps  $\tau$  by the analytic (EGR) propagator and the Haken propagator for the case  $G=1, D=0$  The results show that the Haken propagator is inexact for small  $\tau$ , but becomes increasingly accurate for large  $\tau$

where  $\alpha + \beta = 1$ ;  $\alpha$  and  $\beta$  define the relative importance of  $K$  and  $Q$  at the prepoint  $i$  and the postpoint  $j$ . If  $\alpha = 0$  and  $\beta = 1$ , then  $K$  and  $Q$  are determined at the prepoint; if  $\alpha = 1$  and  $\beta = 0$ , then  $K$  and  $Q$  are determined at the postpoint. If  $\alpha = \frac{1}{2} = \beta$ , then averaged values of  $K$  and  $Q$  are used; this is probably the best choice for most problems with constant or slowly varying  $K$  and  $Q$ , especially if the variation is linear with respect to  $x$ .

*Case 4. Iterative Method.* It is also possible to generate a long-time propagator matrix for any problem by repeated iterations of a short-time propagator matrix upon itself. For example, consider the short-time propagator matrix  $T_{ji}$  of Eq. (1) generated by a finite difference scheme:

$$\bar{N}_j(t_0 + \tau) = \bar{T}_{ji}(\tau) \bar{N}_i(t_0) \quad (16)$$

To find  $\bar{N}_j(t_0 + 2\tau)$ , we can apply  $\bar{T}_{ji}(\tau)$  again:

$$\bar{N}_j(t_0 + 2\tau) = \bar{T}_{ji}(\tau) \bar{N}_j(t_0 + \tau) = \bar{T}_{ji}(\tau) \bar{T}_{ji}(\tau) \bar{N}_i(t_0). \quad (17)$$

If we simply combine the two  $\bar{T}_{ji}$ , then we have a long-time-step-propagator  $\bar{T}_{ji}(2\tau)$ ,

$$\bar{T}_{ji}(2\tau) = \bar{T}_{ji}(\tau) \bar{T}_{ji}(\tau) \quad (18)$$

which satisfies

$$\bar{N}_j(t_0 + 2\tau) = \bar{T}_{ji}(2\tau) \bar{N}_i(t_0). \quad (19)$$

This process can be repeated indefinitely to calculate  $\bar{T}_{ji}(n\tau)$ .

This is a slow and cumbersome method of calculating a long-time-step propagator, but it is accurate, provided that the short time propagator is accurate. It should be noted that although  $\bar{T}_{ji}(\tau)$  may have only a few non-zero elements,  $\bar{T}_{ji}(n\tau)$  should have many non-zero elements

In summary, we have presented four methods of calculating discrete propagators. The EGR and NEGR methods are exact for growth-only problems. The Haken method is nearly exact if the time-steps are moderately large and the  $K$  and  $Q$  terms remain nearly constant. The iterative method is computationally expensive, and its accuracy is limited by the accuracy of the short-time propagator. These methods are analogous to finite-difference schemes, but these methods generally allow larger time-steps. If the propagator matrix is easy to calculate or can be re-used, and if it allows larger time-steps, then these propagator methods are more efficient than finite difference schemes.

## III. PROPAGATORS FOR CONTINUOUS SYSTEMS

Discrete Master equations may be approximated by continuous Fokker-Planck equations of the form

$$\frac{\partial P(x, t)}{\partial t} = -\frac{\partial}{\partial x} [K(x) P(x, t)] + \frac{1}{2} \frac{\partial^2}{\partial x^2} [Q(x) P(x, t)], \quad (20)$$

where  $P(x, t)$  is the probability density of the function (analogous to  $N_x$  in discrete space),  $K(x)$  is the drift velocity, and  $Q(x)$  is the diffusion coefficient. This approximation is good if  $K$  and  $Q$  vary smoothly. Also, the boundary conditions of Section IV are important to force the solution of the Fokker-Planck equation to the solution of the Master equation.

Wehner and Wolfer [1-6] used a path-sum method to calculate a propagator matrix which propagates parts of the function from one grid to another during a time-step  $\tau$ , with an efficiency comparable to a finite difference method.

The propagator matrix has the form

$$T_{j,i}(\tau) = \frac{2}{\Delta x_{j-1} + \Delta x_j} \int_{x_j - \Delta x_{j-1/2}}^{x_i + \Delta x_j/2} dx \int_{x_i - \Delta x_{i-1/2}}^{x_i + \Delta x_i/2} dx_0 \text{Gr}(x, x_0, \tau) \quad (21)$$

and satisfies

$$\bar{P}_j(t_0 + \tau) = \bar{T}_{j,i}(\tau) \bar{P}_i(t_0), \quad (22)$$

where  $x_0$  and  $x$  are the prepoint and postpoint in continuous space,  $\Delta x$  is the width of the histogram, and  $P$  is the height of the histogram (analogous to  $N$  in discrete space).  $\text{Gr}(x, x_0, \tau)$  is a propagator or Green's function which propagates particles from  $x_0$  to  $x$ . There are many propagators which satisfy the Fokker-Planck equation to  $O(\tau^2)$ . The simplest form, given by Dekker [11] is

$$\text{Gr}(x, x_0, \tau) = \frac{1}{\sqrt{2\pi Q(x_0) \tau}} \exp\left(-\frac{(x - x_0 - K(x_0) \tau)^2}{2Q(x_0) \tau}\right). \quad (23)$$

This is very similar to Haken's discrete propagator (see Eq. 13). There are other propagators which also satisfy the Fokker-Planck equation to  $O(\tau^2)$ . For example, the Wissel propagator discussed in Section II may be written in continuous form:

$$T_{j,i}(\tau) = \frac{\exp\left[-\alpha\tau\left(\frac{\partial K(x_j)}{\partial x} - \frac{1}{2} \frac{\partial^2}{\partial x^2} Q(x_j)\right)\right]}{\sqrt{2\pi\tau(\alpha Q(x_j) + \beta Q(x_i))}} \times \exp\left[\frac{\left(x_j - x_i - \tau\left(\alpha K(x_j) + \beta K(x_i) - \alpha \frac{\partial Q}{\partial x}(x_j)\right)\right)^2}{2\tau(\alpha Q(x_j) + \beta Q(x_i))}\right]. \quad (24)$$



The advantage of the Wissel propagator is that for  $\alpha = \frac{1}{2} = \beta$ , the propagator properly weights the values of  $K$  and  $Q$  at both the prepoint and postpoint.

Wehner and Wolfer used a 9-banded matrix which was centered on the diagonal. This meant that a histogram at  $t$  would be propagated to  $i-4, i-3, \dots, i+4$ . This forced a limitation on the time-step:

$$|K\tau| < \sqrt{Q\tau} = \Delta x. \quad (25)$$

In other words, one limitation was that particles should not *drift* more than one grid spacing, since the combined drift and diffusion terms would then propagate a significant part of the function outside the 9 allowed bands.

However, if the 9-banded matrix is centered about the most likely postpoint instead of about the diagonal, then much larger time-steps are allowed; i.e.,  $|K\tau|$  may exceed  $\sqrt{Q\tau} = \Delta x$ . The new limitation on the time-step is that  $K$  and  $Q$  remain nearly constant over the interval from the prepoint to the most likely postpoint  $\bar{x}$ ,

$$\frac{K(x_0)}{K(\bar{x})} = 1 = \frac{Q(x_0)}{Q(\bar{x})},$$

where

$$\bar{x} = x_0 + \int_0^\tau K(x) dt. \quad (26)$$

If  $K$  and  $Q$  are constant independent of  $x$ , then there is *no* limit on  $\tau$  and Dekker's propagator is equivalent to Wissel's. If  $K$  and  $Q$  vary slowly, then Wissel's propagator is usually more accurate than Dekker's propagator, since Wissel's propagator includes  $K$  and  $Q$  at both the prepoint and postpoint.

The efficiency of Wehner and Wolfer's method goes as  $\tau^{3/2}$ , because as  $\tau$  is increased, fewer iterations ( $N$ ) of the propagator are required to find the solution at a later time  $t = N\tau$ , and fewer histograms are used to describe the function, since  $\Delta x = \sqrt{Q\tau}$ .

However, it is not necessary to require that  $\Delta x = \sqrt{Q\tau}$ . If  $\Delta x$  is chosen greater or less than  $\sqrt{Q\tau}$ , then the number of bands in the propagator should be, respectively, decreased or increased to make sure that the propagation from the prepoint is accounted for at all significant postpoints. If the number of bands is too small, then the function will not be conserved and will decrease due to propagation outside the bands. This problem can be alleviated by normalization of the propagator matrix [1-6].

In summary, it is possible to recast the discrete Master equations as a set of continuous Fokker-Planck equations. It is also possible to solve these equations numerically using a propagator method. The efficiency of the method can be increased by choosing an appropriate set of bands in the propagator matrix, which allows a large time-step.

IV. APPLICATION TO THIN FILM NUCLEATION

The discrete propagator methods are now applied to a standard problem in thin film nucleation, Au/NaCl. We show how to include the boundary condition of the problem, which is the deposition of new atoms onto the substrate. Then the analogous continuous propagator methods are also applied to thin film nucleation, and the same boundary condition is used.

In thin film nucleation, several physical processes (deposition, re-evaporation, diffusion, and capture—see Fig. 2) are described by a set of Master equations

$$\begin{aligned} \frac{dN_1}{dt} &= R - \frac{N_1}{\tau_a} - 2N_1G_1 - \sum_{j=2}^{\infty} N_jG_j \\ \frac{dN_2}{dt} &= -G_2N_2 + G_1N_1 \\ &\vdots \\ \frac{dN_i}{dt} &= -G_iN_i + G_{i-1}N_{i-1}, \end{aligned} \tag{27}$$

where  $N_i$  is the number of clusters of  $i$  atoms,  $R$  is the deposition rate of atoms onto the substrate,  $\tau_a$  is the average time before re-evaporation, and  $G_i$  is the capture rate of atoms by clusters of  $i$  atoms. The factor of 2 in the first equation represents the loss of two monomers when they combine to form a dimer.  $G_i$  is given by

$$G_i = \sigma_i D_1 N_1 + \pi r_i^2 R, \tag{28}$$

where  $\sigma_i$  is the capture number for diffusion,  $D_1$  is the diffusion rate of atoms on the substrate, and  $r_i$  is the radius of the cluster. Thus, the first term corresponds to the

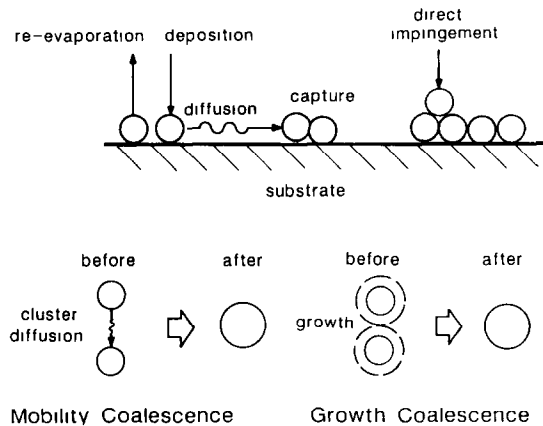


FIG 2 Vapor deposition of atoms onto a substrate

capture of atoms by surface diffusion, and the second term corresponds to the capture of atoms by direct impingement on the cluster. Following the method of Lewis and Anderson [12],  $\sigma_i$  is found by assuming that the system is dilute; i.e., it is calculated by solving both a diffusion equation

$$j(r) = -D_1 \text{grad } N_1(r) \quad (29)$$

and a continuity equation

$$\text{div } j(r) + \frac{\partial N_1(r)}{\partial t} = R - \frac{N_1(r)}{\tau_a}, \quad (30)$$

where  $j$  is the flux. In the steady state,  $\partial N_1(r)/\partial t = 0$ . For the boundary conditions  $N_1(\infty) = R\tau_a$ ,  $N_1(r_i) = 0$ , the solution for the total flux to a cluster  $i$ ,  $J_i$ , is

$$J_i = \frac{2\pi(r_i/\lambda) K_1(r_i/\lambda)}{K_0(r_i/\lambda)} D_1 N_1(\infty), \quad (31)$$

where  $K_0$  and  $K_1$  are zero- and first-order modified Bessel functions, and  $\lambda = \sqrt{D\tau_a}$  is the mean free path before desorption. Since  $\sigma_i = J_i/(D_1 N_1(\infty))$ ,  $\sigma_i$  in Eq. (28) is now defined.

It is possible to solve Eq. (27), using a discrete propagator method. Since it is already assumed that the decay of clusters is negligible, this is a growth-only process which can be described by the EGR and NEGR methods of Section II. Since  $G_i$  varies significantly only for small  $i$ , we use the NEGR method for calculating the propagation of clusters initially smaller than 100 atoms. For clusters with more than 100 atoms, it is possible to use the EGR method using an appropriately averaged  $G_i$ .

$$\bar{G}_i = \frac{1}{2}(G(\text{prepoint}) + G(\text{most likely postpoint})). \quad (32)$$

The propagator methods cannot be used to calculate the boundary condition, which is the nucleation of new islands. However, for dilute systems where  $N_1$  is nearly constant for a time-step  $\tau$ , it is possible to calculate the number of newly nucleated islands. Following the method of Zinsmeister [8], the number of islands  $N_i^0(t_0 + \tau)$ , which nucleated and grew to exactly  $i$  atoms during a time-step  $\tau$  is:

$$N_i^0(t_0 + \tau) = \frac{G_1 N_1}{G_i} \left[ 1 + \sum_{k=2}^i C_{ki} e^{-G_k \tau} \right], \quad (33)$$

where

$$\begin{aligned} C_{ki} &= 1 && \text{for } k = 1 \\ &= C_{k,i-1} \frac{G_i}{G_i - G_k} && \text{for } k \neq i \\ &= - \sum_{s=1}^{i-1} C_{si} && \text{for } k = i. \end{aligned}$$

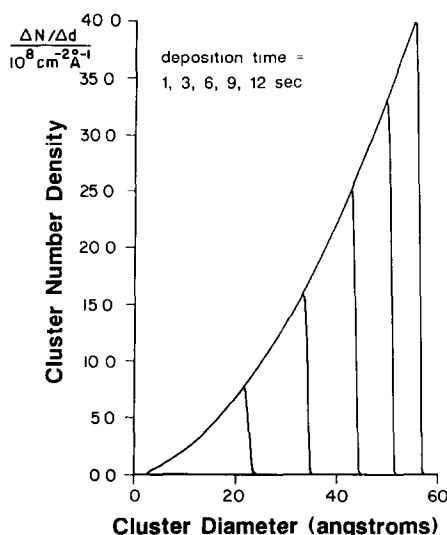


FIG 3 Results of discrete propagator model of the deposition of Au onto NaCl for different deposition times. Mobility coalescence is not included in this model.

In summary, we use the EGR and NEGR methods to calculate the propagation of existing clusters of two or more atoms, and we use Zinsmeister's method to calculate the nucleation rate of new clusters. This yields a set of size distribution histograms, which is graphed as a curve in Fig. 3. Each curve corresponds to the function at a different time.

The same sort of calculation can be done using continuous methods. As with the discrete case, the continuous propagator is used to propagate the existing clusters. Although it is possible to calculate the nucleation of new clusters using continuous boundary condition methods, this is somewhat inaccurate, since the  $G_i$  vary significantly near the boundary which is  $i=1$  for cluster nucleation. It is more accurate to use Zinsmeister's method and then transform those discrete results into continuous form. This yields the nucleation rate of new clusters, and this effect is simply added to the propagation of new clusters. To summarize, we add a discrete solution near the boundary to a continuous solution far from the boundary.

The results of the continuous method are the same as the results of the discrete method (Fig. 3) to within 1%. The discrepancies are largely due to the effect of approximating several discrete points as a single histogram. Since the continuous version used approximately one-third as many grids, it is about three times more efficient. For larger  $\tau$ , the continuous method is increasingly efficient, since fewer grids are used, but this decreases the accuracy.

## V. NONDOMINANT PHYSICAL PROCESSES

In thin film nucleation, the capture of atoms by clusters is the dominant process, and this is a one-step physical process (clusters grow by one atom). However, there are also two possible multi-step physical processes, mobility coalescence and growth coalescence. Mobility coalescence is the diffusion of one cluster to another, where clusters merge to form a single cluster; growth coalescence is the growth of one cluster into another. Growth coalescence becomes very significant when about 40% of the substrate is covered, but mobility coalescence can be significant much earlier if the clusters are mobile.

The experimental size distribution curves measured by Schmeisser [13] give a clear demonstration of mobility coalescence. He deposited Au on NaCl, and observed the effect of coalescence (decrease in total number of clusters and increase in cluster size). Since the total coverage of the substrate was under 5%, mobility coalescence rather than growth coalescence must have been the mechanism.

In this section, we present the results of a computer simulation of Schmeisser's experiments. To incorporate mobility coalescence into the model, it is important to realize that it acts on a much slower time-scale than that of the dominant process (capture of atoms by clusters). Therefore, it is possible to briefly ignore mobility coalescence and use the propagator methods of Sections II and III to evolve the distribution by one time-step. Then the effect of mobility coalescence can be included as a perturbation on the propagator methods.

To determine the rate at which a cluster tends to capture other diffusing clusters, one solves a diffusion equation and a continuity equation. The diffusion equation for the total flux to a disk is

$$J = 2\pi a * D \frac{dC}{dr}, \quad (34)$$

where  $J$  is the total flux of clusters to a cluster,  $D$  is the diffusion rate,  $C$  is the concentration of all the clusters, and  $a$  is the radius of the cluster. The continuity equation assumes a dilute system where capture by other clusters is insignificant,

$$\nabla^2 C = 0 \quad (35)$$

which yields

$$C(r) = A \ln r + B, \quad (36)$$

where  $A$  and  $B$  are unknown coefficients. Two boundary conditions are applied,

$$\begin{aligned} C(a) &= 0 \\ C(R) &= \bar{c}, \end{aligned} \quad (37)$$

where  $R$  is the edge of the Veroni cell defined by  $R = (\pi\bar{c})^{-1/2}$ , and  $\bar{c}$  is the average concentration far from the cluster. This yields

$$C(r) = \frac{\bar{c}}{\ln(R/a)} \ln \frac{r}{a}. \quad (38)$$

Combining Eqs (34) and (37) yields

$$J = 2\pi D \frac{\bar{c}}{\ln(R/a)} \quad (39)$$

which is the rate at which a cluster captures other clusters.

To evolve the cluster distribution efficiently, we group the clusters in large sets, where set 1 has clusters of 2 to 51 atoms, set 2 has clusters of 52–101 atoms, etc. For each set, we determine the number of clusters in the set and the weighted average diffusion rates and size (the numbers of atoms in the cluster). Then the rate of capture of every set by all sets is calculated; this depletes the population of the original sets and creates new clusters. These new clusters are spread proportionately between the two new sets whose average sizes are centered about the average size of the new clusters. After all these calculations are done, then the original cluster population is decreased proportionately according to the proportion of the set which coalesced. Then the population of the new sets are added to the modified population of the original distribution.

This method is far more efficient than individually calculating the rate of coalescence of each cluster size with all possible cluster sizes. However, it is only an approximation which is especially inaccurate when the diffusion rate of the clusters varies dramatically within a set.

It seems that there are two mechanisms responsible for diffusion, both a rapid diffusion mechanism for small islands and a slower diffusion mechanism for large islands. The small island mechanism is probably the random movement of individual atoms in a cluster; this is best illustrated by a dimer whose two atoms continually shift position but remain adjacent to one another. Thus the mobility of small clusters should decrease with increasing cluster size, but the exact relationship is not known, so this mechanism is not included in the model.

The large island mechanism is probably the random movement of the cluster as a whole due to "dislocations" between the island and the substrate. This mechanism should have a diffusion rate which is inversely proportional to the area of the cluster, and this mechanism is included in our model.

In Fig. 4, we display the results of our continuous propagator method which includes mobility coalescence. We found that the best fit to Schmeisser's experimental curves [13] was found by assuming the material parameters

$$\begin{aligned} D_1 &= 3 \times 10^{10} \text{ \AA}^2/\text{s} \\ \tau_a &= 1.5 \times 10^{-7} \text{ s} \\ D_i &= \frac{5 \times 10^{-6} D_1}{i^{2.3}}, \end{aligned}$$

where  $D_i$  is the diffusion rate of a cluster of  $i$  atoms.

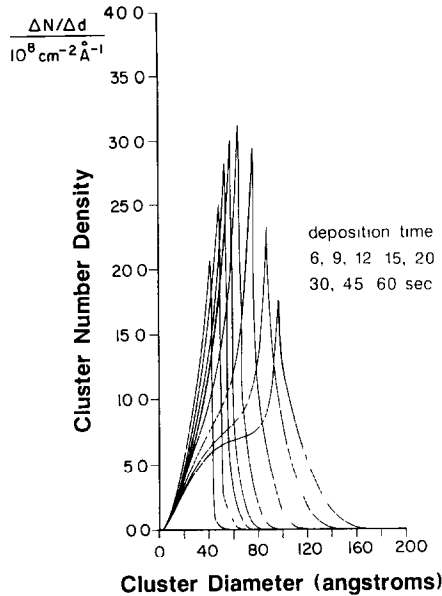


FIG 4 Results of continuous propagator method of the deposition of Au onto NaCl for different deposition times. The physical parameters are the same as in Fig 3, but mobility coalescence is included in this model.

$D_1$  and  $\tau_a$  were found by fitting the position and height, respectively, of the peaks of the curves for 6, 9, 12, 15, and 20 s of deposition. After 20 s, the density of the clusters has increased sufficiently for mobility coalescence to become important. Coalescence decreases the total number of clusters and the number of small clusters, but it increases the number of large clusters.  $D_i$  was found by fitting Schmeisser's 30-, 45-, and 60-s curves, where coalescence is dominant.

The above estimates for  $D_1$  and  $\tau_a$  are probably accurate to within a factor of two. The estimate for  $D_i$  is probably accurate to within a factor of five. The estimate for  $D_i$  does fit the data well, but it is not necessarily the exact relationship of  $t$  to  $D_i$ . Future comparisons with experimental data for different deposition conditions are planned, and those comparisons should determine more clearly the accuracy and predictive ability of this model.

In conclusion, in this section we have shown how slow processes may be accurately treated as perturbations on the basic propagator methods (of Sections II and III) by periodically including the perturbations after one or more applications of the propagator. An example of this is mobility coalescence of islands which predominantly grow by capturing individual atoms. This example yielded realistic estimates of the diffusion and evaporation rates of Au clusters on NaCl.

## VI. SUMMARY

Propagator methods are capable of accurately and efficiently solving both discrete Master equations and equivalent continuous Fokker–Planck equations. Four methods of calculating discrete propagator matrices have been described: the NEGR and EGR methods for growth-only problems; Haken's method for problems with slowly varying growth and decay coefficients, and an iterative method for general problems. For problems in which the growth and decay rates vary slowly in time, these methods allow larger time-steps than explicit finite difference schemes and thus are typically orders of magnitude faster.

The equivalent continuous propagator methods yield nearly identical results to the discrete methods. Also, by decreasing the number of grid points used to describe the function, the continuous method may be increased in efficiency at a modest cost in accuracy. Thus, the continuous method is best for describing the evolution of functions which vary slowly in coordinate space and have many (i.e., thousands) of discrete grid points. The continuous method employed here is much more efficient than finite differences in highly deterministic systems. We have shown how to couple a more accurate discrete boundary condition to the continuous function for certain cases.

Finally, we have applied these propagator methods to a real problem—the nucleation and growth of vapor-deposited thin films. Propagator methods were used to describe the dominant process, the capture of atoms by clusters. Mobility coalescence, a slower process, was periodically included as a perturbation on the process described by propagator methods. By comparison with experimental results, it was possible to quantitatively determine diffusion and re-evaporation rates. These numerical simulations using propagator methods were orders of magnitude faster than an explicit finite difference scheme would have been.

## ACKNOWLEDGMENTS

We thank Dr M Wehner of Lawrence Livermore Labs and Dr W Wolfer of Sandia National Labs for their many useful comments, criticisms, and ideas

## REFERENCES

- 1 M F WEHNER AND W G WOLFER, *Phys Rev A* **27**, 2663 (1983)
- 2 M F WEHNER AND W G WOLFER, addendum to [1]
- 3 M F WEHNER AND W G WOLFER, *Phys Rev A* **28**, 3003 (1983)
- 4 M F WEHNER AND W G WOLFER, *Phys Rev A*, in press
- 5 M F WEHNER AND W G WOLFER, *Philos Mag A* **52**, 189 (1984)
- 6 M F WEHNER, J CHROSTOWSKI, AND W J MIELNICZUK, *Phys Rev A* **29**, 3218 (1984)



- 7 K TAKEUCHI AND K KINOSHITA, *Thin Solid Films* **90**, 27 (1982), *Thin Solid Films* **90**, 31 (1982)
- 8 G ZINSMEISTER, *Vacuum* **16**, 529 (1966).
- 9 H HAKEN, *Z Phys B* **24**, 321 (1976)
- 10 C WISSEL, *Z Phys B* **35**, 185 (1979)
- 11 H DEKKER, *Physica A (Utrecht)* **85**, 363 (1976)
- 12 B LEWIS AND J C ANDERSON, *Nucleation and Growth of Thin Films* (Academic Press, New York, 1978), p 73
- 13 H SCHMEISSER, *Thin Solid Films* **22**, 83 (1974)